Bioactive Materials 14 (2022) 416–429

Contents lists available at ScienceDirect

Bioactive Materials

journal homepage: www.keaipublishing.com/en/journals/bioactive-materials

Fabrication of Tβ4-Exosome-releasing artificial stem cells for myocardial infarction therapy by improving coronary collateralization

Peier Chen [a], Xiaodong Ning [a], Weirun Li [a], Yuxuan Pan [a], Ling Wang [b], Hekai Li [a], Xianglin Fan [a], Jiexin Zhang [a], Tiantian Luo [a], Yaobin Wu [c,**], Caiwen Ou [a,*], Minsheng Chen [a,***]

[a] Guangdong Provincial Biomedical Engineering Technology Research Center for Cardiovascular Disease, Department of Cardiology and Laboratory of Heart Center, Sino-Japanese Cooperation Platform for Translational Research in Heart Failure, Zhujiang Hospital, Southern Medical University, Guangzhou, 510280, China
[b] Biomaterials Research Center, School of Biomedical Engineering, Southern Medical University, Guangzhou, 510515, China
[c] Guangdong Engineering Research Center for Translation of Medical 3D Printing Application, Guangdong Provincial Key Laboratory of Medical Biomechanics, National Key Discipline of Human Anatomy, School of Basic Medical Sciences, Southern Medical University, Guangzhou, 510515, China

ARTICLE INFO

Keywords:
Artificial stem cells
Exosomes
Myocardial infarction
Coronary collateralization

ABSTRACT

Currently, stem cell transplantations in cardiac repair are limited owing to disadvantages, such as immunological rejection and poor cell viability. Although direct injection of exosomes can have a curative effect similar to that of stem cell transplantation, high clearance hinders its application in clinical practice. Previous reports suggested that induction of coronary collateralization can be a desired method of adjunctive therapy for someone who had missed the optimal operation time to attenuate myocardial ischemia. In this study, to mimic the paracrine and biological activity of stem cells, we developed artificial stem cells that can continuously release Tβ4-exosomes (Tβ4-ASCs) by encapsulating specific exosomes within microspheres using microfluidics technology. The results show that Tβ4-ASCs can greatly promote coronary collateralization in the periphery of the myocardial infarcted area, and its therapeutic effect is superior to that of directly injecting the exosomes. In addition, to better understand how it works, we demonstrated that the Tβ4-ASC-derived exosomes can enhance the angiogenic capacity of coronary endothelial cells (CAECs) via the miR-17-5p/PHD3/Hif-1α pathway. In brief, as artificial stem cells, Tβ4-ASCs can constantly release functional exosomes and stimulate the formation of collateral circulation after myocardial infarction, providing a feasible and alternative method for clinical revascularization.

1. Introduction

Myocardial infarction (MI) is a focal necrosis caused by prolonged myocardial ischemia and hypoxia due to coronary obstruction that breaks off the bloodstream [1]. Timely percutaneous coronary intervention (PCI) can remove obstacles from the infarct-related artery, restore local myocardial blood perfusion and reduce the accumulation of harmful metabolites; thereby alleviating cardiomyocyte injury [2,3]. However, due to lack of medical equipment, limited surgical indications, and/or delay in consultation, some patients with MI miss the optimal PCI therapeutic time window, which is closely correlated with prognosis. Effective establishment of collateral circulation after MI can promote the recovery of heart function and shorten hospital stay as well as reduce the incidence of heart failure and death after PCI treatment [4]. At this point, it has attracted great efforts to improve collateral circulation to ameliorate the cardiac function of patients with MI.

Various methods for stimulating angiogenesis and improving coronary collateral circulation, such as stem cell transplantation, biological induction agents, and tissue engineering have been explored in recent years [5–7]. Although the above-mentioned heart regeneration strategies have achieved some success, some problems still exist in clinical practice. For example, immunological rejection, short residence time, or poor cell viability after stem cell transplantation, may greatly hinder its application [8,9]. Moreover, the injection of biological induction agents can cause pathological angiogenesis and allergic reactions [10]. A single delivery of cytokines has also been tested for cardiac therapeutic effects

Peer review under responsibility of KeAi Communications Co., Ltd.
* Corresponding author.
** Corresponding author.
*** Corresponding author.
E-mail addresses: wuyaobin2018@smu.edu.cn (Y. Wu), oucaiwen@smu.edu.cn (C. Ou), gzminsheng@vip.163.com (M. Chen).

https://doi.org/10.1016/j.bioactmat.2022.01.029
Received 7 November 2021; Received in revised form 16 January 2022; Accepted 17 January 2022
Available online 29 January 2022

in clinical trials. Thymosin β4 (Tβ4), a key pro-angiogenic factor, can induce epicardial ancestor cells to differentiate into endothelial cells, improving the formation of new blood vessels [11,12]. A single infusion of intramyocardial Tβ4 can reduce tissue damage and improve cor-onary collateralization after MI [13,14]. However, this approach cannot achieve the desired effect because of its inability to deliver nucleic acid molecules and proteins to target cells for angiogenesis.

Recently, genetically modified stem cell-derived exosomes have been receiving increasing attention in the biomedical field because of their unique advantages in stimulating angiogenesis [15]. Such engineered exosomes can regulate the gene expression of angiogenesis-related pathways in target organs by delivering bioactive substances, such as microRNAs (miRNAs) [16–18]. This regulation has a positive effect on the state and function of endothelial cells, in terms of cell viability, migration, and tube formation capacity, which can enhance angiogenesis in the infarction zone [19]. Thus, there are grounds to believe that Tβ4 gene-transfected mesenchymal stem cell-derived exosomes (Tβ4-EXO) can promote coronary collateralization and have great application prospects in cardiac repair. In addition, due to high incidence of cardiovascular diseases, there is an urgent need to improve continuous transmission of exosomes to cardiomyocytes. However, to significantly promote angiogenesis with the help of exosomes is challenging because of poor retention in the myocardial infarcted area.

Encapsulating exosomes within hydrogels, that can be easily injected because of their low viscosity, might be a good way to achieve sustained release [20,21]. However, the release rate of exosomes in this way is usually rapid and uncontrollable, and hence, cannot meet the requirements of continuous administration. Hydrogels with high viscosity might show higher retention of exosomes, but it would be rather difficult to inject them. Therefore, searching for another drug supporter that can achieve the purpose of sustained release of exosomes is essential. Microspheres produced by microfluidic technology have aroused great interest for their multiscale structures, functional characteristics, and injectable capability [22,23]. They have been widely used to deliver drugs, growth factors, and nanophase materials in the medical field [22,24]. What's more, a previous report showed that monodisperse microspheres can continuously release kartogenin over five weeks to repair articular cartilage degeneration, which may make it an ideal exosome carrier [25].

In this study, we attempted to fabricate injectable Tβ4-exosome-releasing artificial stem cells (Tβ4-ASCs) using microfluidics technology to integrate photo-cross-linkable gelatin methacryloyl (GelMA)/polyethylene (glycol) diacrylate (PEGDA) matrix with Tβ4-EXO (Fig. 1). Tβ4-ASCs can continuously release Tβ4-EXO in the infarcted area for treatment, which are attributed to the sustained release capacity of the microspheres. In addition, such artificial stem cells can greatly reduce the

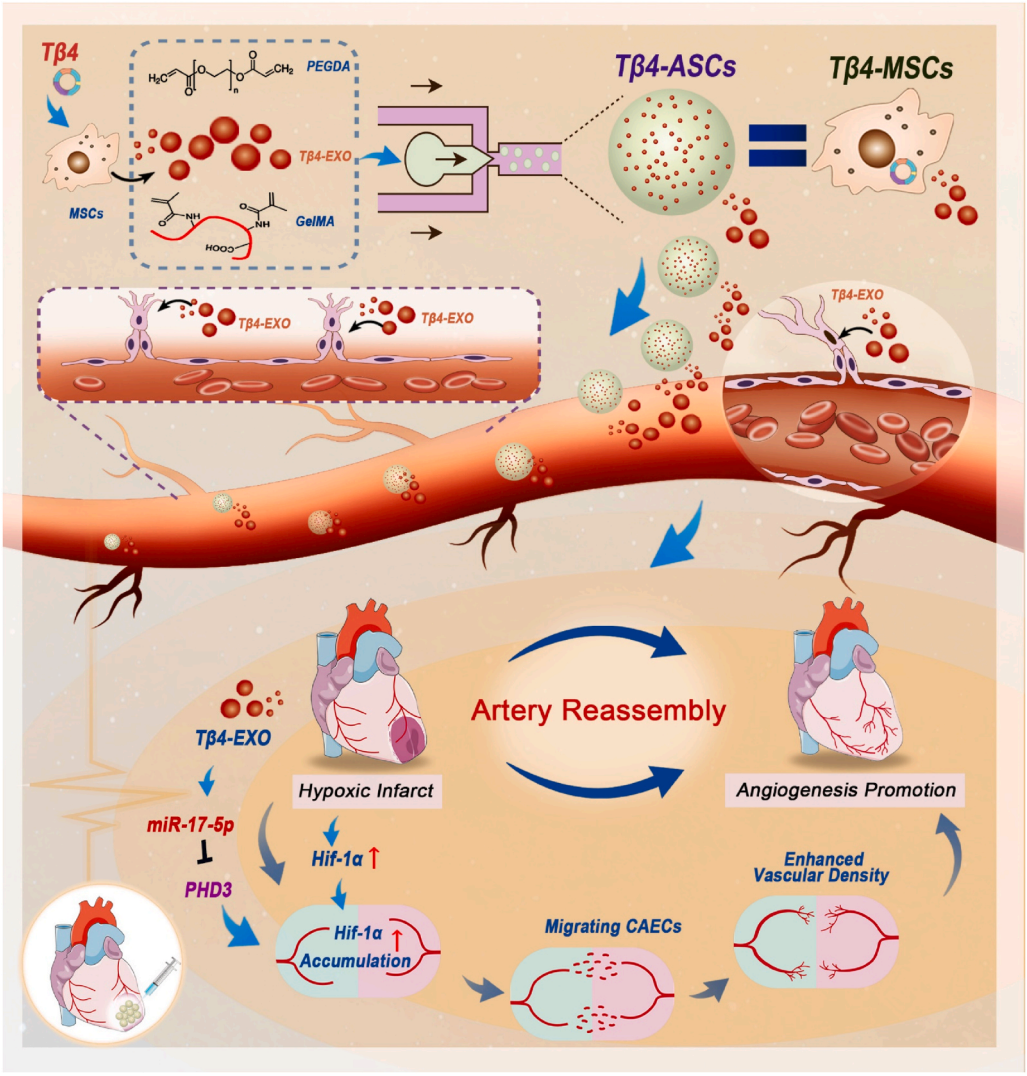

Fig. 1. Schematic diagram illustrating the assembly of engineered artificial stem cells (Tβ4-ASCs) and cardioprotective effect for their sustained release of Tβ4-exosomes in myocardial infarcted area.

risk of tumorigenesis and immunogenicity associated with the transplantation of stem cells. Although there are many studies on how exosomes work, their mechanisms remain unclear. Some studies have shown that the hif-1α signaling pathway plays an important role in coronary collateralization [26,27]. Based on this, we speculated that the therapeutic effects of Tβ4-EXO may have an intimate connection with that signaling pathway. Collectively, functional artificial stem cells, called Tβ4-ASCs, which can repair ischemic tissue, have great potential for application in the biomedical field, especially in myocardial regeneration.

2. Materials and methods

2.1. Cell culture

Mouse bone marrow–derived MSCs were isolated and cultured as described previously [28]. Briefly, bone marrow was harvested via repeated washing of the tibia cavity; then, the aspirate was centrifuged at 1000 rpm for 5 min. The cell containing pellets were resuspended in DMEM/F12 (Gibco, USA), supplemented with 10% fetal bovine serum (FBS) and 1% penicillin-streptomycin (Gibco, USA), plated on 6-well cell culture clusters, and cultured at 37 °C in a 5% CO_2 constant-temperature incubator (Thermo, USA). Coronary endothelial cells (CAECs) were purchased from the Procel life science Laboratory (Wuhan, China), and cultured in endothelial cell medium (Sciencell, USA) supplemented with 10% fetal bovine serum (FBS) and 1% penicillin-streptomycin (Gibco, USA) at 37 °C in a 5% CO_2 constant-temperature incubator (Thermo, USA).

2.2. Exosome isolation, identification, and labeling

After culturing MSCs in exosome-free medium for 48 h, the supernatant was collected. First, the sample was centrifuged at 300×*g* for 10 min. This was followed by ultracentrifugation at 2000×*g* for 10 min. This was followed by ultracentrifugation at 10,000×*g* for 30 min. The cells, membranes, and debris were discarded. The supernatant was then filtered through a 0.22 μm filter (Merck Millipore). Finally, 120,000×*g* ultracentrifugation was performed for 90 min. The exosomes were resuspended in PBS and washed at 120,000×*g* for 90 min. The microstructure of the exosomes was observed using transmission electron microscopy (TEM). Nanoparticle tracking analysis (NTA) was used to measure the diameter and number of particles in exosomes. The zeta potentials of exosomes were measured using a Zetasizer Nano ZS90 analyzer (Malvern, UK). The protein content of exosomes was measured using bicinchoninic acid (BCA) protein assay (Thermo Scientific, USA), and exosome markers were detected using Western blot (1:1000, Abcam). The labeled PKH-26 exosomes were washed at 120,000×*g* for 60 min to remove unlabelled PKH-26 exosomes. The PKH-26 kit was used in accordance with the manufacturer's instructions (Sigma-Aldrich).

2.3. Oxygen-glucose deprivation (OGD) model in CAECs

CAECs were cultured in a 37 °C hypoxic (1% O_2, 5% CO_2) incubator in sugar-free DMEM (Gibco, USA) for 6 h to induce ischemic injury. For treatment, CAECs were treated with exosomes for 12 h at 50 μg/mL.

2.4. Immunohistochemistry

For 30 min, the cells were fixed in 4% paraformaldehyde. The cells were rinsed three times with PBS and permeabilized for 10 min with 0.5% Triton-100. After completing the aforementioned protocols, the cells were washed three times with PBS and incubated with 3% BSA for 30 min. The primary antibodies were incubated at 4 °C overnight. The following primary antibodies were applied: Tβ4 (1:500 dilution, Affinity), Hif-1α (1:500 dilution, CST), VEGF-A (1:500 dilution, CST), CD31 (1:500 dilution, Abcam), and α-SMA (1:500 dilution, CST). Next, the cells were rinsed five times in PBS before being titrated with an appropriate secondary antibody (1:800 dilution, Abcam) and incubated at room temperature for 1 h. At last, the cells were stained with DAPI for 5 min following rinse with PBS and laser confocal microscopy was used to examine the images.

2.5. Tube formation on Matrigel

80 μL Matrigel (Corning, USA) was added to each well of a 24-well plate and incubated for 30 min in a common incubator. 80 μL of the cell suspension was added to each well after coagulation. There was approximately 3×10^4 cells in total. After 6–8 h, the cells were examined under a microscope. The length of the capillary structure was measured using ImageJ software to determine tube formation.

2.6. Migration assay

In a 6-well plate, 5×10^5 cells/well were planted and cultured to confluence for the wound healing assay. The core monolayer of CAECs was scraped with a pipette tip and rinsed with a serum-free solution to remove unattached cells. CAECs were imaged at 0, 12, and 24 h after injury. The migration area to calculate wound closure was calculated as follows: migration area (%) = (A0–An)/A0 × 100%, where A0 represents the initial wound area and an represents the wound area at the time of measurement. Cells (3×10^4 cells/well) were suspended in a low-serum (0.5% FBS) mixture and inserted with a pore size of 8 μm (FALCON, USA) in a 24-well plate for the transwell assay. The cells that adhered to the upper surface of the filter were removed after 24 h, and the cells that migrated were stained with 0.1% crystal violet on the lower surface. Cell migration was determined using an optical microscope.

2.7. RNA extraction and real-time PCR

Total RNA was isolated from samples using TRIzol reagent (AG, China) and reverse transcribed to first-strand cDNA using conventional methods (AG, China). RT-qPCR was also carried out under the following conditions: initial denaturation at 95 °C for 30 s, denaturation at 95 °C for 5 s, and annealing/extension at 60 °C for 30 s for 40 cycles. Primers sequences used for qRT-PCR were showed in supporting information Table S1.

2.8. Western blot analysis

The expression of the following proteins was detected using Western blot: Alix (1:1000 dilution, Abcam), CD9 (1:1000 dilution, Abcam), Syntenin-1 (1:1000 dilution, Abcam), Tβ4 (1:1000 dilution, Affinity), GAPDH (1:1000 dilution, Bioworld), Hif-1α (1:1000 dilution, Abcam), VEGF-A (1:1000 dilution, Abcam), ANG I (1:1000 dilution, Abcam), and ANG II (1:1000 dilution, Abcam). A suitable amount of protein sample was obtained for electrophoresis at constant pressure, transferred to a polyvinylidene difluoride membrane (Millipore, USA), and placed in a protein-blocking solution (Beyotime, China) at room temperature for 1 h. The membrane was incubated overnight with a primary antibody at 4 °C. On the second day, the membrane was incubated with horseradish peroxidase (HRP)-labeled secondary antibody (1:5000 dilution, Bioworld), agitated gently at room temperature for 1 h, washed, and developed with an enhanced fluorochemiluminescent system, after repeated washing. Images were observed and captured using the color fluorescence imaging technology.

2.9. Preparation of GelMA/PEGDA hydrogel

GelMA was synthesized via the reaction of gelatin with methacrylic anhydride (MA), as described in our previous study [29]. In brief, gelatin

was completely dissolved in DPBS at a concentration of 10% (w/w) at 60 °C. MA was then added to the gelatin solution at a rate of 0.5 mL/min. The mixture solution was allowed to react for 3 h at 50 °C, followed by dialysis (Mw = 5000 Da) against distilled water for several days. The solution was then lyophilized for 3 days to obtain a white porous GelMA foam maintained at −80 °C. The structure of GelMA was characterized by HNMR as seen in Fig. S2. To prepare the GelMA/PEGDA hydrogel, GelMA and PEGDA were completely dissolved in DPBS solution to obtain a GelMA/PEGDA solution with a final concentration of 75 mg/mL each. LAP (0.2% w/v) was added to the solution as the photoinitiator. Polyethylene (glycol) diacrylate (PEDGA) (Mw = 700 Da) was purchased from Sigma-Aldrich (Lot: 455008) and used without further purification.

2.10. Fabrication of microfluidic chip

On a glass slide, the microfluidic chip had two inlets and a single outflow. A round capillary glass tube and a square quartz tube with inner diameters of 150 and 500 μm, respectively, were used as inlets. The internal diameter of the conical tip on the round capillary glass tube was fixed at 30 μm. A centrifuge tube was used to collect microspheres at the exit.

2.11. Preparation of Tβ4-EXO GelMA/PEGDA microsphere

Tβ4-EXO loaded GelMA/PEGDA microspheres were prepared on the above-mentioned microfluidic chip. Tβ4-EXOs were mixed with GelMA/PEGDA precursor solution at a ratio of 1:4 to obtain a water phase solution containing Tβ4-EXO at a final concentration of 1 mg/mL. The oil phase solution was prepared using mineral oil containing 5% (v/v) Span 80. The water phase solution and the oil phase solution were injected at the I1 and I2 inlets, respectively; the complex solution droplets (water-in-oil) were formed at the conical head and came from the O outlet. The Tβ4-EXO loaded microspheres were formed after exposure to 365 nm UV irradiation in the middle of the silicone tube. Subsequently, the Tβ4-EXO loaded microspheres thus formed were collected in a tube and centrifuged to collect them (see Movie 1). To visualize the distribution of EXOs, the Tβ4-EXOs were pre-stained with PKH26 (red), and the GelMA/PEGDA precursor solution was pre-treated with FITC (green).

Supplementary video related to this article can be found at https://doi.org/10.1016/j.bioactmat.2022.01.029

2.12. Sustained release of Tβ4-ASCs in vitro

To determine the release kinetics of PKH26 labeled exosomes from Tβ4-ASCs, Tβ4-ASCs were incubated in test tubes containing 1 mL of PBS. The tubes were gently shaken in a rotating incubator at 37 °C. The mixture was centrifuged at 3000×*g* for 5 min. Next, 500 μL supernatant was sampled from the tubes and supplemented with the same amount of PBS. The concentration of PKH26-labeled exosomes was measured using a fluorescence spectrophotometer. PKH26-labeled exosomes packed in microspheres were injected in vivo, into the infarcted myocardial border zone. Frozen sections were used to detect exosome retention in the hearts on day 1, 4, 7, 14, and 21 after microsphere injection. Fluorescence microscopy was used to view and analyze cells.

2.13. MI model in mice

The Animal Research Committee at Southern Medical University approved the animal care and experimental techniques. C57BL/6 mice (18–25 g, 6–8 weeks) were anesthetized with a 50 mg/kg sodium pentobarbital intraperitoneal injection and ventilated by tracheal intubation. The thoracic cavity was opened to expose the heart after shaving and cleaning. 8-0 nylon sutures were used to ligate the left anterior descending coronary arteries of the mice. ST-segment elevation on the ECG verified the MI model.

2.14. MR imaging of coronary artery flow

Gadopentetic acid (Gd-DOTA), a contrast agent, was injected through tail vein. T1 flash and PCA sequence were used to scan contrast-enhanced coronary artery under respiration and ECG gating (TR 21.7 ms; TE 5.7 ms). Finally, the post-image processing was analyzed by using the software 3D slicer.

2.15. Retrograde perfusion of mouse coronary vasculature

Coronary vasculature was conducted as described previously [30]. Briefly, the Microfil® injection conpounds (MV-122) was perfused into the aortic root and allowed to spread throughout the coronary vasculature.

2.16. Exosome small RNA sequencing

The purified small RNA fragment of the sample was extracted, and the 3′ and 5′ connectors were successively connected to reverse transcription into cDNA, following which PCR amplification was performed. Then, the target fragment library was recovered by glue cutting, and the qualified library was sequenced by Illumina HiSeq™2500 platform (Ribobio, China).

2.17. Luciferase reporter assay

293T cells were cultured in 96-well plates to 60% confluence, then co transfected with either miR-17-5p expression vector or mutant PHD3 3′UTR vector. After 48 h, the Dual-Glo® Luciferase Assay System (Promega, USA) was used to determine the luciferase activity of each group.

2.18. Statistical analysis

Data were analyzed using GraphPad Prism 9.0 (GraphPad Software Inc, USA). Two groups were compared using the *t*-test analysis, and three or more groups were analyzed using one-way analysis of variance (ANOVA). Values with a P value less than 0.05 ($P < 0.05$) were considered significant.

3. Results

3.1. Preparation and characterization of Tβ4-ASCs

The separation and identification of bone marrow-derived mesenchymal stem cells (MSCs) are illustrated in Fig. S1. The expression of Tβ4 was much higher in Tβ4-MSCs than in Nor-MSCs after lentiviral transfection, which corresponded to the results of Western blot and immunofluorescence, indicating that Tβ4 was successfully transfected into MSCs (Fig. 2a–b). The required exosomes obtained from different media were then characterized by transmission electron microscopy (TEM) and nanoparticle tracking analysis (NTA). The exosomes were typical cup-shaped membrane vesicles with a diameter of approximately 100 nm, as seen in the TEM image. TEM results indicated that the overexpression of Tβ4 did not impair the morphology of exosomes (Fig. 2c). The diameters of Nor-EXO and Tβ4-EXO ranged from 50 to 150 nm, which is consistent with the previously reported exosome size distribution (Fig. 2d). Moreover, the extracted exosomes were highly enriched with exosome-specific marker protein (including Alix, CD9, CD81 and syntenin-1) [31] and overexpression of Tβ4 in Tβ4-EXO according to the Western blot analysis (Fig. 2e). We then used zeta sizer to examine the membrane potential of exosomes and the data showed the membrane potential had no remarkable difference between Nor-EXO and Tβ4-EXO (Fig. 2f–g). The exosomes can be taken up inside cells through direct fusion and endocytosis pathways and participate in many biological actions, like immune response, as an essential medium of intercellular

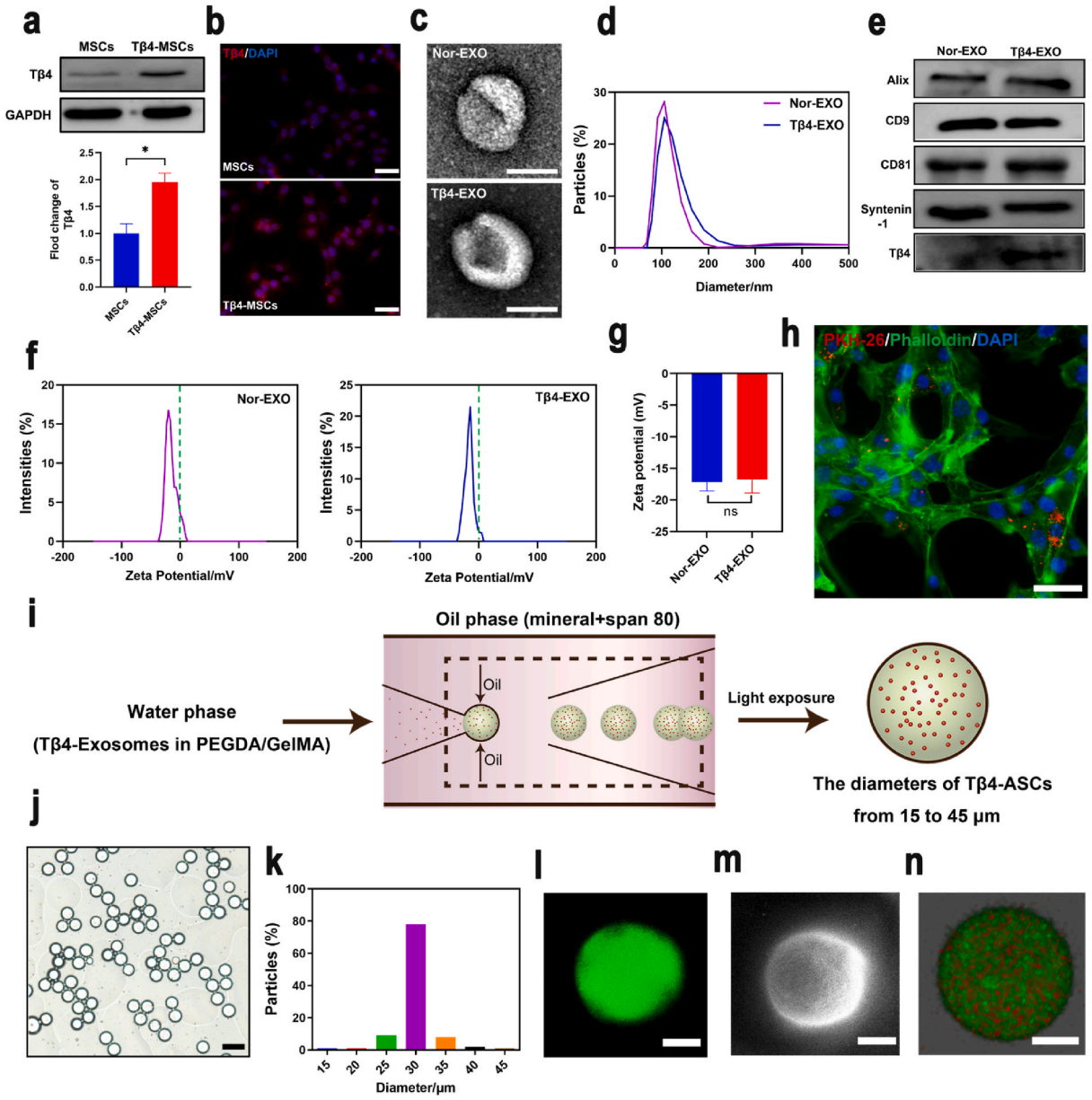

Fig. 2. Preparation and characterization of Tβ4-ASCs. (a) The expression of Tβ4 in MSCs and Tβ4-MSCs was detected via Western blot respectively. *P < 0.05. (b) The expression of Tβ4 in MSCs and Tβ4-MSCs were detected via immunofluorescence respectively. (c) TEM imaging of Nor-EXO and Tβ4-EXO. Scale bar = 100 nm. (d) The average diameter and distribution of Nor-EXO and Tβ4-EXO was detected via NTA analysis. (e) The expression of exosomal markers (Alix, CD9, CD81, Syntenin-1) and Tβ4 in Nor-EXO and Tβ4-EXO were detected via Western blot. (f) Images of zeta potential measurements. (g) Quantitative evaluation of zeta potential measurements. (h) PKH-26-labeled exosomes (red) were taken up by CAECs (green) in vitro, as shown by confocal imaging. Scale bar = 50 μm. (i) The schematic design of Tβ4-ASCs preparation. (j) The surface morphology of Tβ4-ASCs was observed under an optical microscope. Scale bar = 50 μm. (k) Particle size of Tβ4-ASCs. (l) Fluorescence image of Tβ4-ASCs. Scale bar = 15 μm. (m) SEM photograph of Tβ4-ASCs. Scale bar = 15 μm. (n) 3D fluorescence view of Tβ4-ASCs. Scale bar = 15 μm.

communications. Here, PKH-26, a type of lipophilic dye, was used to confirm the cellular uptake of specific exosomes. As shown in Fig. 2h, PKH26-labeled exosomes (red) were found in the cytoskeleton of phalloidin + CAECs (green) in confocal images, implying that exosomes can bring biologically active substances to CAECs for treatment. All these results suggest that required exosomes were successfully prepared and proven to be taken up inside cells like cellular uptake of exosomes secreted by cells under physiological conditions. Next, we prepared Tβ4-exosome-releasing artificial stem cells (Tβ4-ASCs) by encapsulating Tβ4-EXO within microspheres via microfluidics technology. Fig. 2i shows the schematic design of the preparation of Tβ4-ASCs. Simply put, the desired microsphere droplets with a diameter of approximately 30 μm can be acquired with the help of microfluidic technology by adjusting the ratios of the oil phase flow rate and Tβ4-EXO/GelMA/PEGDA solution (Fig. 2j–k, Fig. S3, Movie 1). Tβ4-ASCs were further characterized by fluorescent staining and SEM. As shown in Fig. 2m–n, the obtained Tβ4-ASCs were spherical and uniform in size with a smooth surface. According to the three-dimensional (3D) views of the fluorescent staining images (Fig. 2n), Tβ4-EXOs (red) were evenly distributed in the microspheres (green), indicating that Tβ4-EXOs have been successfully encapsulated in the microspheres. These results demonstrate that Tβ4-ASCs were successfully prepared by using microfluidic technology.

3.2. Improvement in the angiogenic capacity of the coronary endothelial cells in vitro with the help of exosomes derived from Tβ4-ASCs

As shown in Fig. S4, the addition of GW4869 inhibitor that can reduce exosome secretion to the conditioned medium partially reversed the protective effect. Surprisingly, Tβ4-conditioned medium significantly reduced apoptosis of CAECs and enhanced cell viability under oxygen glucose deprivation (OGD). In our study, Tβ4-ASCs mainly exerted a therapeutic effect by releasing exosomes, similar to that of the paracrine secretion of Tβ4-MSCs. Hence, in the following cell experiments, Tβ4-EXOs were directly used to intervene with CAECs under OGD to determine the protective effect of Tβ4-ASCs. With the pretreatment of Tβ4-EXO for 12 h, CAECs presented higher survival rate under OGD compared to other interventions (Fig. 3a). Cell migration, transwell (8 μm), and tube formation experiments were used to study the effects of Tβ4-EXO on angiogenesis. As shown in Fig. 3b–c, CAECs migrated to the scratched region over time, and that co-cultured with Tβ4-EXO migrated faster at 12 and 24 h than those cultured with Nor-EXO. The number of migrating CAECs increased considerably following incubation with Tβ4-EXO, as validated by the transwell (8 μm) assay (Fig. 3d–e). Tβ4-EXO's angiogenesis-stimulating impact was investigated in vitro using a tube-like structure creation experiment. As shown in Fig. 3f–h, the intervention group treated with Tβ4-EXO had a larger number of branch nodes and tube formations compared to the group treated with Nor-EXOs, which was consistent with the results of the CAECs migration assay. The nitric oxide (NO) gas produced by endothelial cells can regulate tension in blood vessels and inhibit platelet or leukocyte adhesion [32]. Therefore, we further examined the total content of NO in conditioned media collected from different treatment groups. As can be seen from Fig. 3i, when the total NO content in the blank control

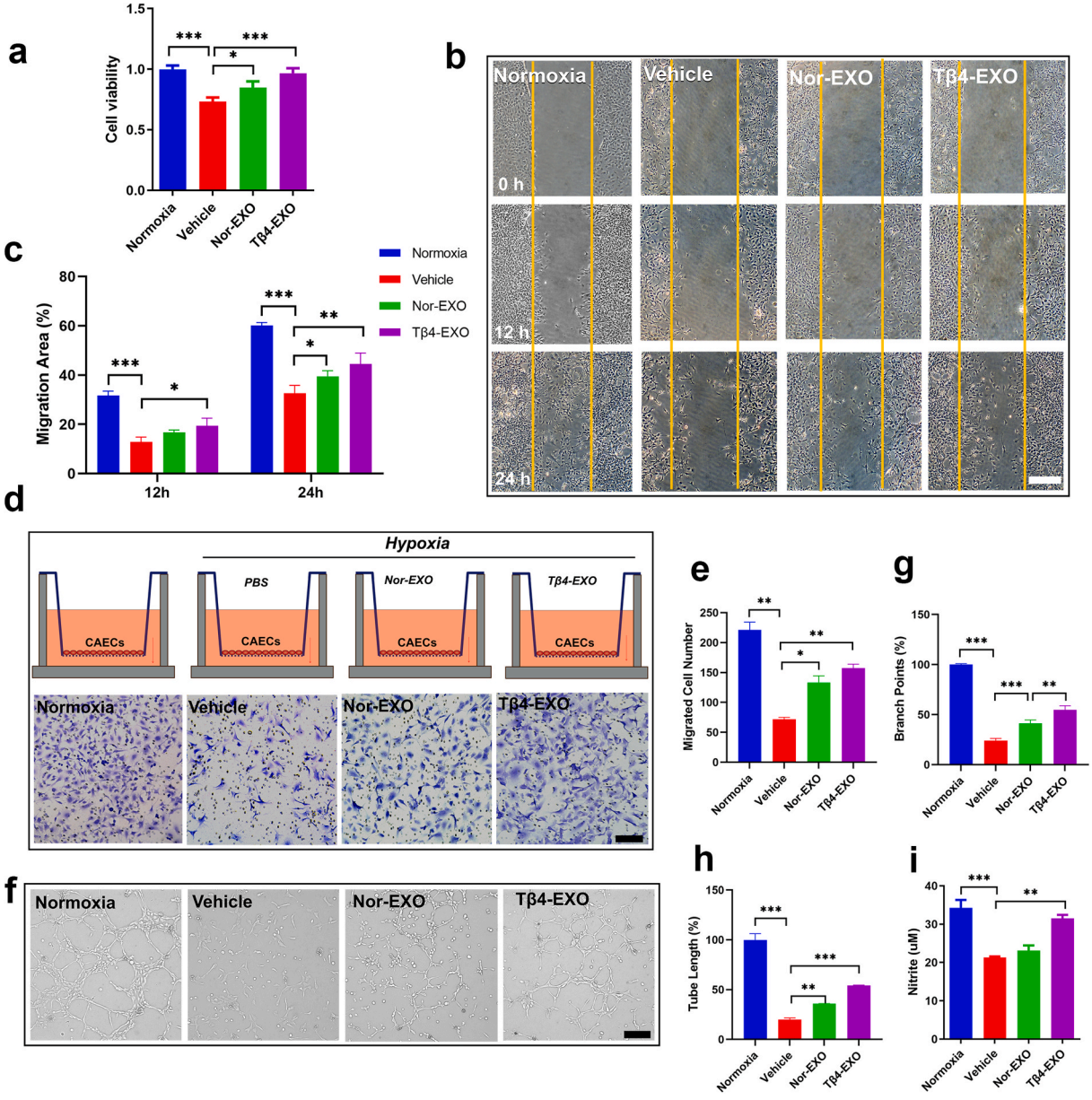

Fig. 3. Tβ4-EXO promoted CAECs angiogenesis. (a) Viability of CAECs treated with Nor-EXO and Tβ4-EXO after OGD. *P < 0.05; **P < 0.01; ***P < 0.001. (b) Wound-healing assay for different treatments. (c) Quantitative evaluation of wound-healing assay. *P < 0.05; **P < 0.01; ***P < 0.001. (d) Transwell assay for different treatments. (e) Quantitative evaluation of the transwell assay. *P < 0.05; **P < 0.01. f) Tube formation on Matrigel under different treatments. (g, h) Quantitative assay of tube formation on Matrigel. *P < 0.05; **P < 0.01; ***P < 0.001. Scale bar = 250 μm. (i) Total content of nitrogen monoxide (NO) in the culture media collected from different CAECs treatments. **P < 0.01; ***P < 0.001.

group decreased sharply under OGD, and treatment with Tβ4-EXOs significantly increased the production of NO in CAECs. In addition, flow cytometry (FCM) analysis showed that treatment with Tβ4-EXOs markedly reduced CAECs apoptosis under OGD, as illustrated in Fig. S5. To further confirm the capacity of Tβ4-EXOs to promote angiogenesis, qRT-PCR analysis and immunofluorescence cell staining were also performed (Fig. S5). According to qRT-PCR analysis, Tβ4-EXO enhanced the expression of angiogenic-related genes, including ANG-I, ANG-II, IGF-1, and HGF, as compared to Nor-EXO. Next, CD31, a marker of vascular endothelial cells, was labeled by immunofluorescence staining to observe the formation of microvessels (Fig. S5). These results suggest that Tβ4-EXO helps CAECs form blood vessels against OGD, which

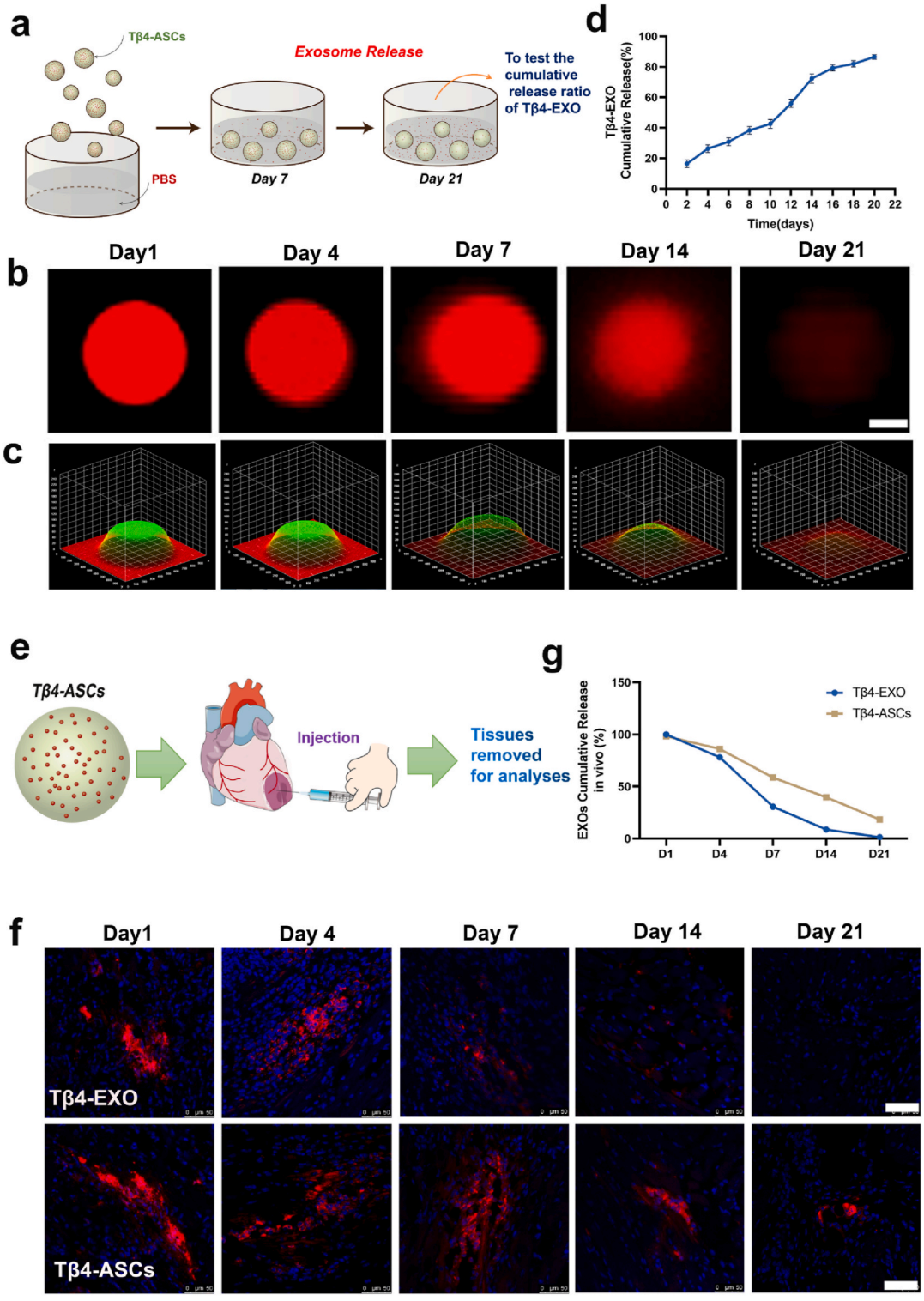

Fig. 4. The sustained-release ability of Tβ4-ASCs. (a) The sustained release scheme of exosomes of Tβ4-ASCs in vitro. (b, c) Tβ4-ASCs confocal fluorescent microscopy images and their overall gray level of each 3D surface plot: From Day 1 to Day 4, Day 7, Day 14, Day 21, the fluorescence intensity dropped as the release time increased. Scale bar = 15 μm. (d) A fluorescence spectrophotometer was used to measure the cumulative release ratio of Tβ4-EXO with PKH26 labelling. (e) The sustained release scheme of exosomes of Tβ4-ASCs in vivo. (f, g) The release behavior of Tβ4-ASCs in vivo.

indicated that exosomes released from Tβ4-ASCs can do this as well.

3.3. The sustained-release of Tβ4-ASCs

The exosomes release behavior of Tβ4-ASCs was investigated in PBS at 37 °C for three weeks to assess the paracrine function of artificial stem cells (Fig. 4a). As shown in Fig. 4b–c, and Fig. S6, the fluorescence intensity of Tβ4-ASCs decreased as time elapsed, indicated by the overall gray level of each 3D surface plot. This confirms that Tβ4-EXO can be released continuously from the microspheres. Fig. 4d further illustrates the sustained release ability of Tβ4-ASCs for the release curve of Tβ4-EXOs in vitro over a period of 21 days. Next, Tβ4-EXOs were specifically labeled with PKH-26 to investigate the controlled release effect of Tβ4-ASCs in vivo (Fig. 4e). When PKH26-Tβ4-EXO was injected directly, the fluorescence signal of Tβ4-EXO disappeared within 14 days. But PKH26-Tβ4-EXO encapsulated in Tβ4-ASCs remained detectable even after 21 days (Fig. 4f–g). Simultaneously , the vitro imaging showed that the fluorescence of PKH26-Tβ4-EXO can be detected in the heart 7 days after operation, which means effective accumulation of Tβ4-EXO in the heart instead of other organs (Fig. S7). The longer the residence time of exosomes in the myocardium, the greater effect of the treatment. Besides, Tβ4-ASCs presented a reliable biosafety in vivo base on the decrease of fluorescence intensity of inflammatory marker CD68 in MI area, which was further confirmed by the hepatic and renal function examinations on animal models (Fig. S8). Together, all these data demonstrated that Tβ4-ASCs can continuously release functional Tβ4-EXOs to tissues such

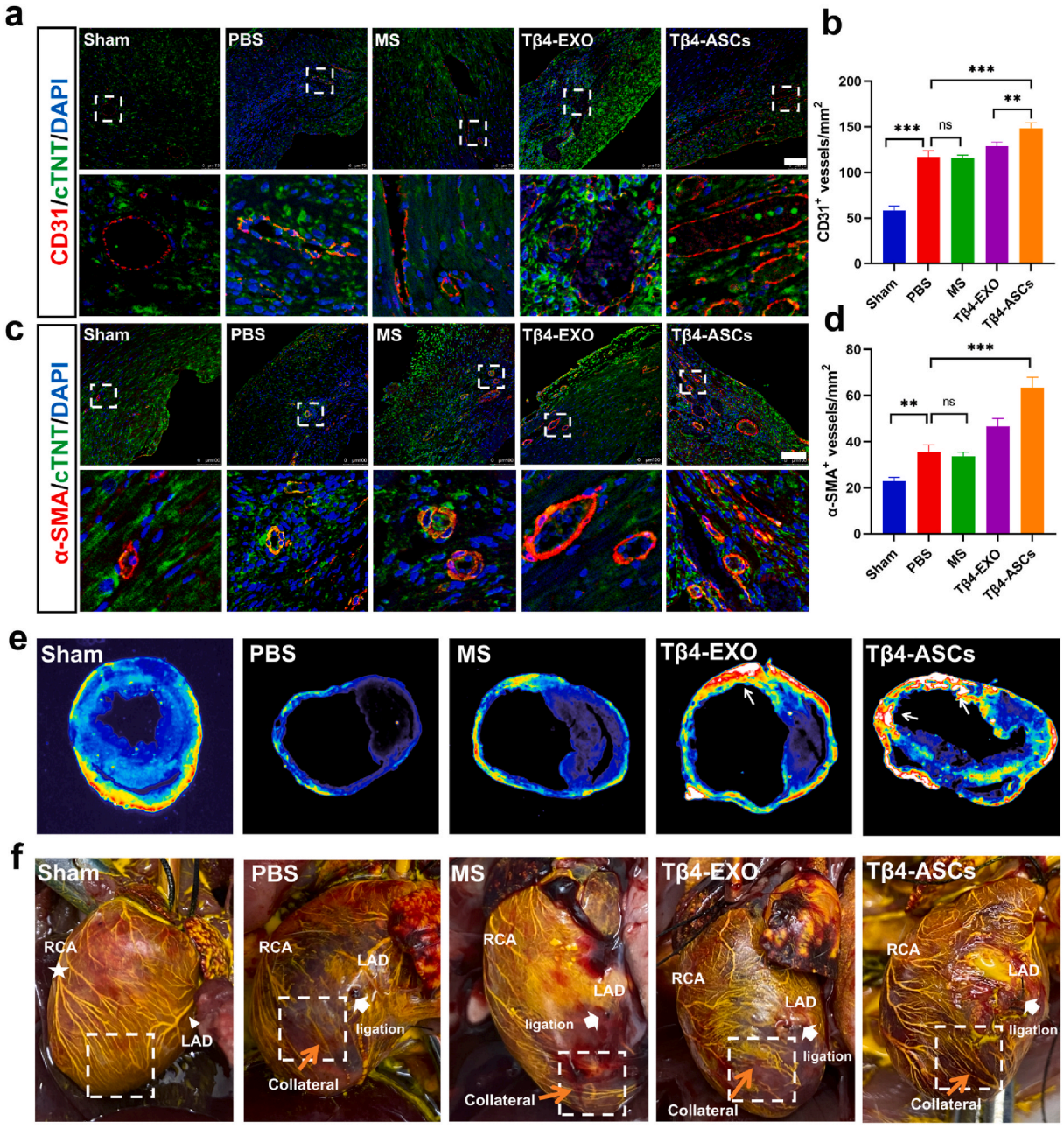

Fig. 5. Tβ4-ASCs improved coronary collateralization after myocardial injury. (a) Representative of CD31 staining in heart tissues. Scale bar = 75 μm. (b) Quantification analysis of CD31 positive vessel-like structures number. **P < 0.01; ***P < 0.001. (c) Representative of α-SMA staining in heart tissues. Scale bar = 100 μm. (d) Quantification analysis of α-SMA positive vessel-like structures number. **P < 0.01; ***P < 0.001. (e) The whole cross-section of the heart displaying CD31 expression in its entirety. (f) Representative of microfilled hearts. White star-RCA: right coronary artery; White triangle-LCA: left anterior descending; White arrow-the ligation of LAD.

as stem cells that secrete cytokines. The stem cell therapy has attracted a lot of attention mainly because the stem cells from different sources can release various cytokines, especially exosomes, in response to tissue injury. Thus, fabrication of artificial stem cells by combining Tβ4-EXO from Tβ4-MSCs and microspheres provides an effective and stable strategy for its application as a potential alternative to stem cell therapy.

3.4. MI therapy performance of Tβ4-ASCs

Promoting coronary collateralization is essential to rebuild the supply of nutrients and oxygen to the ischemic area to increase the survival rate of cardiomyocytes after MI. In animal experiments, immunofluorescence analysis revealed that Tβ4-ASCs treatment greatly increased the vascular densities compared to just microspheres (MS) treatment or the mixture of MS and Tβ4-EXO on day 28 (Fig. 5a–d, Fig. S9). The whole of horizontal heart sections through a near-infrared laser imager and immunohistochemistry experiment also confirmed that Tβ4-ASCs therapy raised the expression levels of CD31 (Fig. 5e). Cardiovascular magnetic resonance (CMR) was used to assess endothelial damage and neovessel formation in injured coronary arteries [33]. Fig. S10 shows that the contrast enhancement of vessel was better in the Tβ4-ASCs treatment than that in the Tβ4-EXO treatment. The results of CMR corresponded well to the cell migration and tube formation of CAECs (Fig. 3b–f), indicating that Tβ4-ASCs can spur further formation of coronary collateral circulation in vivo. The retrograde perfusion of coronary vasculature was used to vividly observe coronary collateral circulation in vivo. Due to the ligation of left anterior descending (LAD), the vascular density in infarcted region decreased. While Tβ4-EXO and Tβ4-ASCs treatment appeared to promote the formation of collateral circulation between the right coronary arteries (RCA) and LAD, Tβ4-ASCs treatment had a better effect (Fig. 5f). Moreover, the results of TUNEL assay demonstrated that apoptosis-positive cells were scattered throughout the cardiac tissue slices of mice, and Tβ4-ASCs treatment significantly reduced cell apoptosis at the myocardial injury site, as shown in Fig. 6a–b. Next, Masson's trichrome staining was used to analyze fibrosis staging of the myocardium. The results showed that both Tβ4-ASCs and Tβ4-EXO treatment can help prevent myocardial fibrosis and cardiac remodeling (Fig. 6c–e). However, the difference was that the therapeutic effect of the former was better and more satisfactory. Echocardiography was performed to detect the systolic and

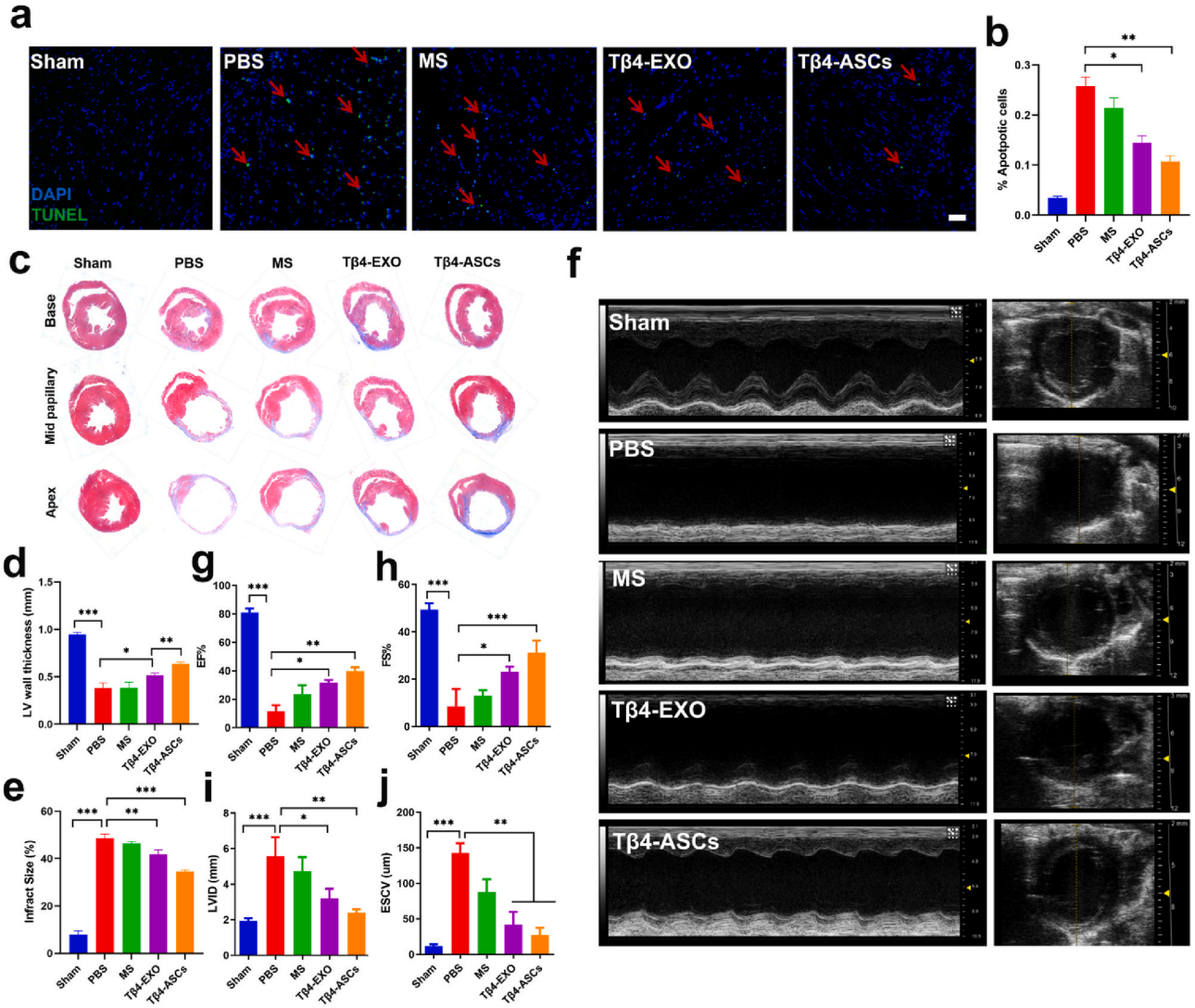

Fig. 6. Tβ4-ASCs improved cardiac function following myocardial injury. (a) TUNEL staining showed apoptosis in the different treatment groups on day 28 after MI. (b) Quantification of apoptosis in different treatment groups. *P < 0.05; **P < 0.01. (c) Masson's trichrome staining indicated the degree of cardiac fibrosis in different treatment groups on day 28 after MI. (d) Quantitative assay of infarct wall thickness. *P < 0.05; **P < 0.01; ***P < 0.001. (e) Quantitative assay of infarct size. **P < 0.01; ***P < 0.001. (f–j) Representative M-mode images and quantification of EF%, FS%, ESCV and LVID measured via echocardiography of sham, PBS, microsphere, Tβ4-EXO, and Tβ4-ASCs treatment on day 28 after MI. *P < 0.05; **P < 0.01; ***P < 0.001.

diastolic functions of the heart (Fig. 6f). In contrast to PBS and Tβ4-EXO treatment, treatment with Tβ4-ASCs significantly improved the ventricular systolic function, as evidenced by higher ejection fraction (EF%) and fraction shortening (FS%) (Fig. 6g–h). Furthermore, the end-systolic chamber volume (ESCV) and end-systolic left ventricular internal diameter (LVID) on echocardiography post treatment with Tβ4-ASCs were better than those of the other two groups, indicating that Tβ4-ASCs can effectively prevent left ventricular remodeling after MI (Fig. 6i–j). The animals experiment results demonstrated that Tβ4-ASCs can effectively promote collateralization and improve cardiac function.

3.5. *The mechanism of Tβ4-ASCs derived exosomes mediated collateralization and cardiac repair*

Further studies are needed to investigate the mechanism of Tβ4-ASCs derived exosomes (Tβ4-EXO) in improving collateralization and cardiac function. The hypoxic environment may cause Hif-1α to dimerize with Hif-1β, resulting in an increased production of VEGF-A [34]. To explore the influence of Tβ4-EXO on the Hif-1α/VEGF-A axis further, immunofluorescence labeling was used to detect Hif-1α and VEGF-A expression in CAECs (Fig. 7a–b). The ratio of Hif-1α/DAPI in CAECs was considerably higher in the Tβ4-EXO than in the Nor-EXO treatment, as shown in Fig. 7c. The ratio of VEGF-A/DAPI was similar to that of Hif-1α/DAPI (Fig. 7d). These findings suggest that the capacity to induce CAECs to form small branches of the coronary artery may be related to the upregulation of Hif-1α and VEGF-A genes. This hypothesis was further validated by qRT-PCR and Western blot analysis, as shown in Fig. 7e–i. To understand the effect of Tβ4-EXOs on CAECs angiogenesis better, expression of other angiogenesis-related genes, such as Ang I and Ang II were also studied. Ang I and Ang II increased slightly in the Tβ4-EXO treatment compared to the other groups, as seen in Fig. 7j–k. In summary, these data suggest that Tβ4-EXO can facilitate the expression of Hif-1α and VEGF-A to promote the formation of coronary collateral circulation.

Exosomes are a type of secretory extracellular vesicles (EVs) that deliver biologically active molecules (including microRNAs) to mediate in cell-to-cell communication. Thus, we hypothesized that Tβ4-EXO-delivered miRNA may be responsible for CAECs angiogenesis in Tβ4-ASCs. A total of 108 differentially expressed miRNAs ($P < 0.05$; Fig. 8a) between Tβ4-EXO and Nor-EXO were detected using Illumina HiSeq 2500 high-throughput sequencing, and analyses of gene expression profiles suggested that Tβ4-EXO enhanced CAECs angiogenesis via up-

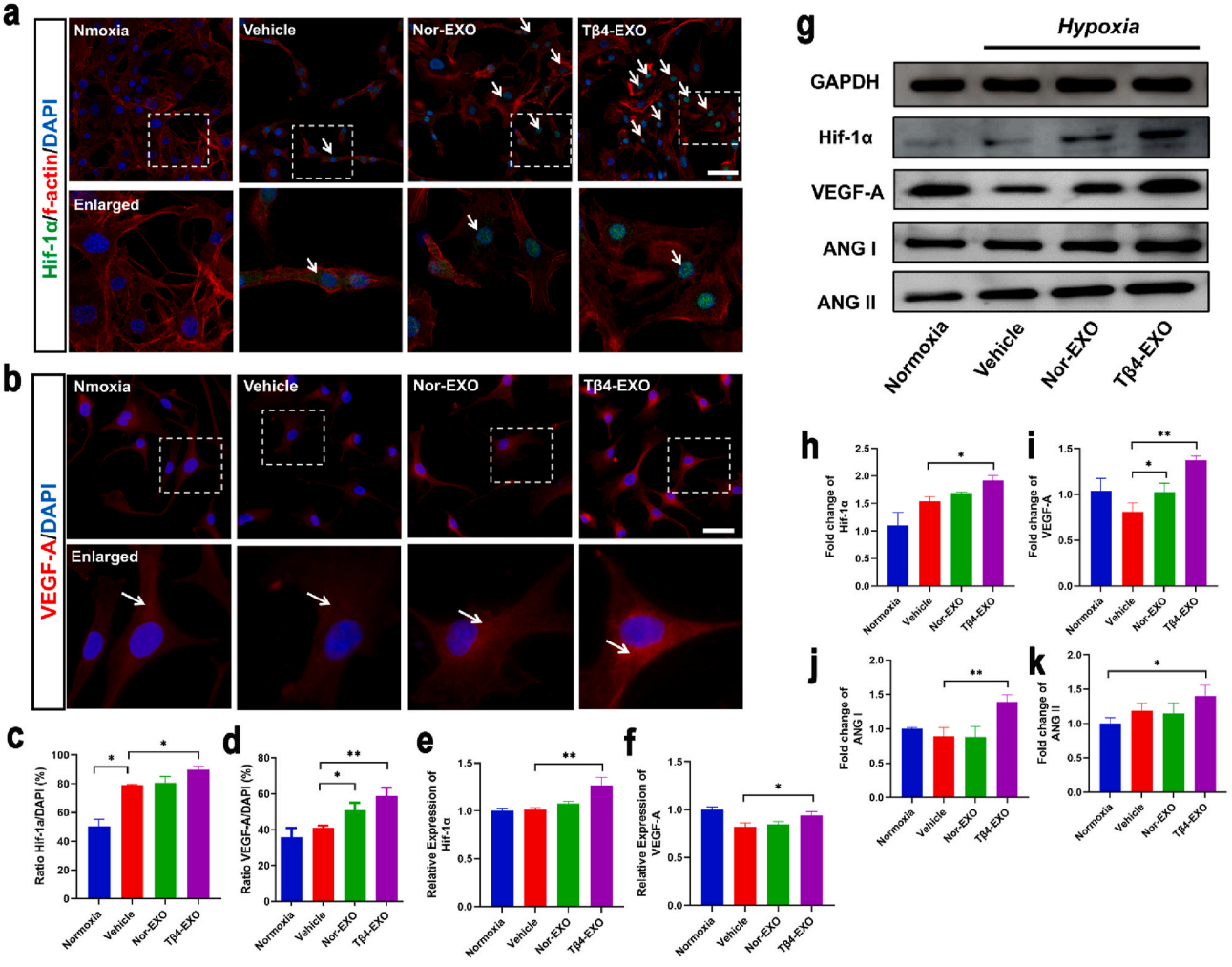

Fig. 7. Tβ4-ASCs derived exosomes promote CAECs angiogenesis by stabilizing Hif-1α and activating VEGF-A after OGD. (a) Hif-1α (green), F-actin (red), and DAPI (blue) expressions were detected using an immunofluorescence staining technique. Scale bar = 50 μm. (b) The expression of VEGF-A (red) and DAPI (blue) was detected using an immunofluorescence staining technique. Scale bar = 50 μm. (c) Expression of Hif-1α in CAECs after OGD. *P < 0.05. (d) VEGF-A expression in CAECs after OGD. *P < 0.05; **P < 0.01. . (e, f) The qRT-PCR analysis of Hif-1α and VEGF-A in CAECs cocultured with different types of EXOs. *P < 0.05; **P < 0.01. (g) Hif-1α, VEGF-A, ANG I and ANG II protein expression was evaluated via Western blot analysis in CAECs treated with Nor-EXO and Tβ4-EXO. (h) Quantitative assay for Hif-1α protein expression. *P < 0.05. (i) Quantitative assay of VEGF-A protein. *P < 0.05; **P < 0.01. (j) Quantitative assay of ANG I protein. **P < 0.01. (k) Quantitative assay of ANG II protein. *P < 0.05.

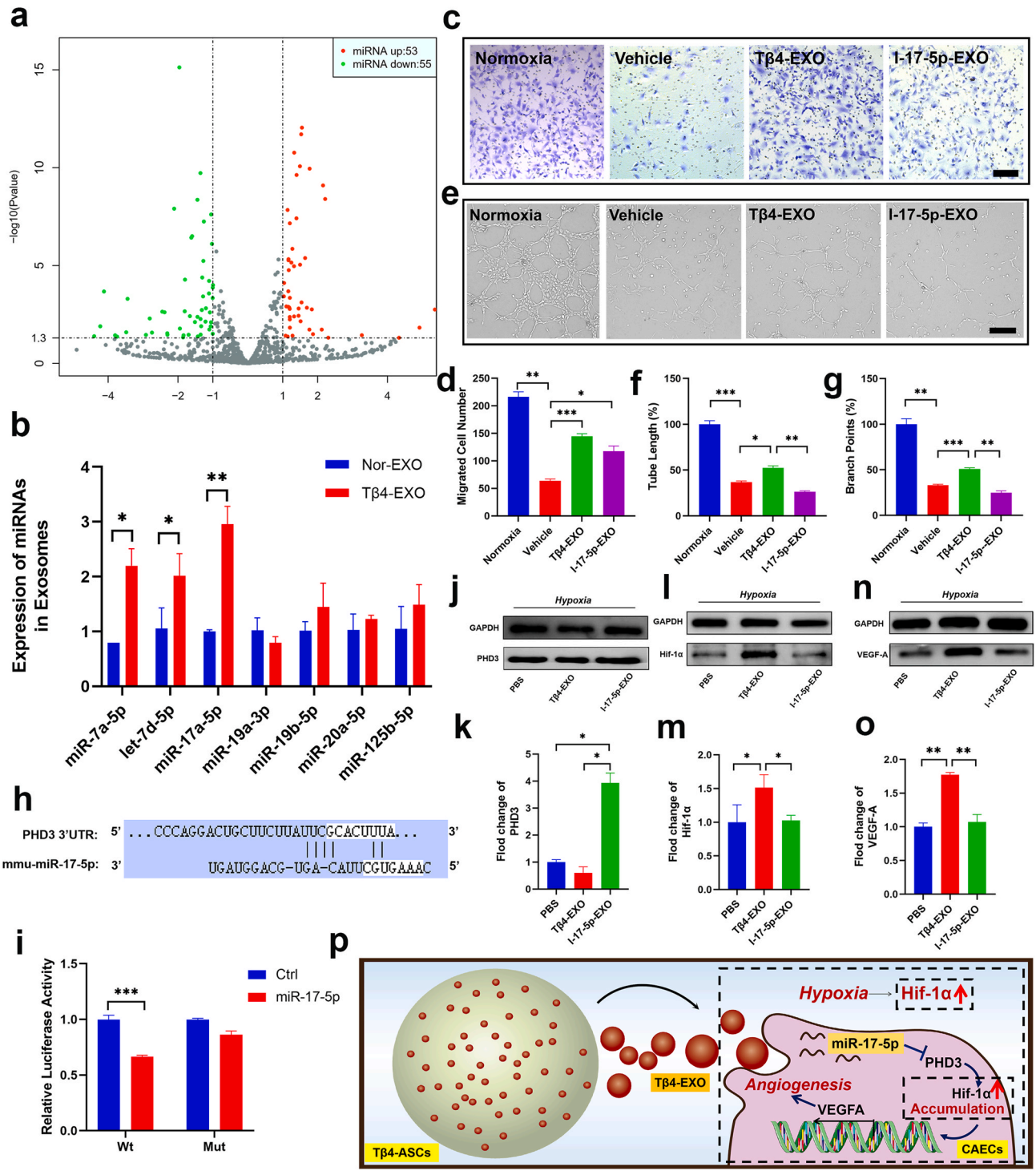

Fig. 8. miR-17-5p transferred by Tβ4-EXO mediating in angiogenesis. (b) A comparison of seven differently expressed miRNAs in Nor-EXO and Tβ4-EXO using qRT-PCR. Data were normalized to spiked cel-miR-39. *P < 0.05; **P < 0.01. (c) The transwell assay. Scale bar = 250 μm. (d) The transwell assay quantitative evaluation. *P < 0.05; **P < 0.01; ***P < 0.001. (e) Tube formation on Matrigel. Scale bar = 250 μm. (f, g) Tube formation on Matrigel in a quantitative experiment. *P < 0.05; **P < 0.01; ***P < 0.001. (h) A bioinformatics investigation revealed that PHD3 is a possible miR-17-5p target gene. (i) The luciferase assay system was used to determine the luciferase activity of each group. ***P < 0.001. (j, k) The expression of PHD3 protein was detected via Western blot. *P < 0.05. (l, m) The expression of Hif-1α protein was detected via Western blot. *P < 0.05. (n, o) The expression of VEGF-A protein was detected via Western blot. **P < 0.01. (p) The scheme of Tβ4-EXO-miR-17-5p on angiogenesis in hypoxic conditions.

regulating the VEGF-A pathway activity (Fig. S11). As shown in Fig. 8b, three of the seven differentially expressed miRNAs were upregulated in the Tβ4-EXO group compared to that in the Nor-EXO group. Next, three miRNAs selected above were detected by miRNA-specific qRT-PCR analysis. The findings demonstrated that MSCs transfected with lentivirus-mediated Tβ4 elevated miR-17-5p expression levels as compared to controls, but there were no significant differences in miR-7a-5p or let-7d-5p expression in MSCs between the two groups. Furthermore, after Tβ4-EXO therapy, miR-17-5p expression in CAECs increased considerably (Fig. S12). Collectively, Tβ4-EXOs may mediate

in CAECs angiogenesis by transferring miR-17-5p. We used inhibitor transfection to knock down miR-17-5p in MSCs to further investigate the promotion of angiogenesis effect of miR-17-5p delivered by exosomes and detected the angiogenesis ability of exosomes isolated from miR-17-5p knockdown MSCs in CAECs. CAECs treated with exosomal-miR-17-5p knockdown showed dramatically decreased migratory potential in transwell assays and wound healing assays (Fig. 8c–d, Fig. S13). The tube formation assay revealed that exosomal-miR-17-5p knockdown decreased both the number of branching points and the formation of tube structures (Fig. 8e–g). Collectively, the Tβ4-EXO transfer of miR-17-5p affects angiogenesis.

In addition, potential downstream targets of miR-17-5p that contribute to endothelial cell angiogenesis, especially under hypoxic conditions, were predicted using bioinformatics and online prediction databases. These results suggest that prolyl hydroxylase 3 (PHD3), a hydroxylase of Hif-1α proteasomal degradation, may be a potential target for its 3′-untranslated region (UTR) with miR-17-5p binding sites (Fig. 8h). Next, a luciferase assay system was used to further determine the binding sites for miR-17-5p in the 3′-UTR of PHD3. The data suggest that miR-17-5p mimic reduced luciferase activity for PHD3 of wild-type 3′-UTR rather than PHD3 of mutant-type 3′-UTR (Fig. 8i), which confirms that PHD3 was the downstream target of miR-17-5p. The previous research has shown that reduced PHD3 activity under hypoxic conditions can enhance Hif-1α stabilization, nucleocytoplasmic translocation, and dimerization with the Hif-1α subunit, to initiate the transcription of certain angiogenic genes (e.g., VEGF) [35]. Next, as shown in Fig. 8j–k, we found an obvious increase in PHD3 expression at the protein level following the transfection of CAECs with suppressed miR-17-5p. In addition, Western blot analysis confirmed that miR-17-5p elevated the expression of Hif-1α and VEGF-A (Fig. 8l–o). These findings implied that Tβ4-EXOs may promote CAECs angiogenesis through PHD3 repression to facilitate Hif-1α stability and VEGFA expression (Fig. 8p).

4. Discussion

There are many collateral branches between the coronary artery and its branches, which are regarded as potential conduits. The early development of collateral coronary artery, also known as collateral circulation, is closely related to the improvement of survival rate in patients with MI [36,37]. In the present study, we developed a strategy to promote coronary collateralization by constructing artificial stem cells (Tβ4-ASCs), which are capable of continuously releasing Tβ4-exosomes. Our results demonstrated that Tβ4-ASCs can constantly release functional exosomes and effectively stimulate the formation of collateral circulation via the miR-17-5p/PHD3/Hif-1α pathway after MI. The construction of such “artificial stem cells” has great potential for application in the biomedical field, especially in myocardial regeneration, as it offers an alternative method to induce coronary collateralization. Moreover, to our knowledge, there have been very few reports on the construction of artificial stem cells to repair ischemic myocardial tissue and the effects of Tβ4-EXO on the formation of coronary collateral circulation.

Stem cell therapy faces many challenges in clinical applications [8,38]. First, the viability of transplanted stem cells in the host is very low; second, there is a potential risk of immune rejection in cell transplantation, and direct intramuscular injection or intravenous administration of stem cells could increase the risk of thromboembolism. Nevertheless, experimental and clinical studies have shown that stem cell transplantation still has an obvious therapeutic effect on MI. Increasing evidence shows that adult stem cells play a therapeutic role mainly through their paracrine biological effects rather than by direct differentiation [39,40]. Among them, exosomes have cardioprotective functions similar to stem cells, which can promote angiogenesis and improve cardiac function. However, by further study, the pitfalls of exosome therapy for myocardial injury are being gradually exposed [41–43]. They are as follows: 1) poor tissue targeting, 2) low quantity of effective therapeutic components, and 3) low concentration of effective therapeutic components. To address these shortcomings, researchers have prepared customized exosomes artificially to achieve therapeutic goals. Here, we found that preparation of artificial stem cells which can simulate the paracrine behavior of adult stem cells and achieve sustained release of exosomes would be advisable and possible. Driven by this, we applied microfluidic technology to prepare injectable Tβ4-exosome-releasing artificial stem cells (Tβ4-ASCs) with a diameter of 30 μm. PEGDA has been widely used to produce microspheres for sustained drug delivery owing to its excellent mechanical strength, and drug loading, and release ability [44,45]. GelMA segments were added to obtain microspheres with improved mechanical properties and biodegradability [46,47]. The sustained release of Tβ4-EXO in the microspheres was achieved by free diffusion and degraded release at the same time, similar to the paracrine function of stem cells; we called it Tβ4-Exosome-Releasing Artificial Stem Cells (Tβ4-ASCs). More importantly, Tβ4-ASCs can continuously release exosomes in the infarction zone in vivo for more than 21 days.

In animal experiments, we demonstrated that Tβ4-ASCs significantly enhanced blood flow in the ischemic heart on day 28. At the same time, we also evaluated the level of neovascularization after MI. The results showed that Tβ4-ASCs can significantly increase the number of new small branches of the coronary artery, which further confirmed that Tβ4-ASCs can promote the formation of coronary collateralization to restore blood supply to the myocardial infarcted area. What’s more, the result of Masson’s trichrome staining proved that Tβ4-EXO released from Tβ4-ASCs can reduce the myocardial fibrosis, and the cardiac function was improved with the treatment of Tβ4-ASCs, which was validated by echocardiography.

In our study, the customized exosomes were isolated from Tβ4 gene-transfected MSCs through differential ultracentrifugation in accordance with the previously described methods. In EXOs, the quantity of mature miRNAs is approximately 41.7% of the total RNA [48]. EXOs containing miRNAs can be transported to recipient cells and used to regulate gene expression post-transcriptionally [49]. To explore which miRNAs are involved in Tβ4-EXO-mediated angiogenesis, we performed a miRNA profiling assay to compare the differences between Tβ4-EXO and Nor-EXO using Illumina HiSeq 2500 high-throughput sequencing. Seven (miR-7a-5p, let-7d-5p, miR-17-5p, miR-19a-3p, miR-19b-5p, miR-20-5p, and miR-125b-5p) of the 108 differentially expressed miRNAs were further confirmed via qRT-PCR analysis. We found that Tβ4 lentiviral transfection notably upregulated miR-17-5p expression in MSCs, and then this particular miRNA was transferred into exosomes with the secretion of stem cells. Previous studies have demonstrated that the miR-17–92 cluster can improve the angiogenic capacity of endothelial cells [50], and miR-17-5p, a component of the miR-17–92 cluster, can activate the angiogenic ability of endothelial cells in vitro in cell-autonomous manner [51]. The miR-17-5p knockdown was accomplished by transient transfection to further test the angiogenic ability of Tβ4-EXO transferred miR-17-5p on angiogenesis. The suppression of miR-17-5p drastically inhibited tube formation and migration of CAECs, as well as the expression of angiogenic-related genes, indicating that miR-17-5p was closely related to Tβ4-EXO-mediated angiogenesis. Hif-1α is the main transcription factor involved in the adaptive response to hypoxic condition [52]. Concurrently, Prolyl-4 Hydroxylase Domain (PHDs) are the key molecules that regulate Hif-1α levels, especially PHD3 [53]. PHD3 can hydroxylate the specific proline residues in amino-terminal ODD region of Hif-1α, and then the hydroxylated modified Hif-1α quickly binds to the pVHL (von Hippel-Lindau) protein, which finally can be degraded by ubiquitin-proteasome system [54,55]. In hypoxic conditions, reduced PHD activity promotes Hif-1α stabilization, translocation to the nucleus and dimerization with the Hif-1α subunit, triggering the transcription of several angiogenic genes [56]. In our study, Tβ4-EXO can enhance the expression of exosomal-miR-17-5p which can reduce Hif-1α ubiquitination by targeting PHD3. Simultaneously, this suppressive effect of miR-17-5p on PHD3 is beneficial for

the accumulation of Hif-1α in hypoxic conditions. Hence, Tβ4-ASCs-derived exosomes can stimulate angiogenesis via miR-17-5p/PHD3/Hif-1α pathway.

There are a few things to note. The location of Tβ4 in exosomes was not explored in this study due to conditionality. Thus, we don't know whether Tβ4 located in exosomes lumen or outer membrane or both. If we want to further clarify the expression of Tβ4 in exosomes, the immunogold TEM analysis would be recommended to detecte [57,58]. Besides, we used just adult bone marrow mesenchymal stem cells (BM-MSCs) derived exosomes for Tβ4-ASCs preparation. Although MSCs appear to be well tolerated and have unique immunologic characteristics, the restricted capacity for proliferation and impaired differentiation potency that will increase batch-to-batch variation of MSCs-derived exosomes with culture passages will hinder its further application [59,60]. Recently, a clinical study has shown that GMP-grade MSCs derived from induced pluripotent stem cells (iPSCs) (CYP001) are associated with better outcomes in refractory graft-versus-host-disease (GVHD) [61]. Although much more needs to complete the human clinical trials of iPSC-derived cells, their capacity for multilineage differentiation and indefinite proliferation possibly make them to be ideal alternative sources of MSCs, especially in exosomes production. This will be one of the works we are going to carry out next.

5. Conclusions

To mimic the paracrine and biological activity of stem cells, we successfully developed artificial stem cells (Tβ4-ASCs), which can continuously release Tβ4-exosomes, by combining microspheres and treated exosomes. Tβ4-EXOs released constantly from Tβ4-ASCs can greatly enhance the angiogenic capacity of CAECs, playing a vital role in coronary collateralization. In an experiment conducted on mice, we find that Tβ4-ASCs have a superior therapeutic effect and can safely improve cardiac function by inducing the formation of branches of the coronary artery. Moreover, in mechanistic studies, we demonstrate that Tβ4-ASC-derived exosomes improved collateralization via the miR-17-5p/PHD3/Hif-1α pathway under hypoxic conditions. Hence, with the sustained release of functional exosomes in situ, Tβ4-ASCs can effectively induce the formation of collateral circulation after MI, providing a feasible alternative method for clinical revascularization.

Data availability

The raw/processed data forms part of an ongoing study and may be requested from the authors.

CRediT authorship contribution statement

Peier Chen: Conceptualization, Writing – original draft, Data curation. **Xiaodong Ning:** Conceptualization, Data curation. **Weirun Li:** Writing – original draft. **Yuxuan Pan:** Methodology, Data curation. **Ling Wang:** Writing – review & editing. **Hekai Li:** Methodology, Software. **Xianglin Fan:** Methodology. **Jiexin Zhang:** Validation. **Tiantian Luo:** Software. **Yaobin Wu:** Conceptualization, Writing – review & editing. **Caiwen Ou:** Conceptualization, Writing – review & editing, Funding acquisition. **Minsheng Chen:** Conceptualization, Writing – review & editing, Funding acquisition.

Declaration of competing interest

The authors declare that they have no known competing financial interests or personal relationships that could have appeared to influence the work reported in this paper.

Acknowledgements

This study was supported by grants from the National Natural Science Foundation of China (No.81971765, 31771060, 31671025, 81871504, 32171355 and 82172103).

Appendix A. Supplementary data

Supplementary data to this article can be found online at https://doi.org/10.1016/j.bioactmat.2022.01.029.

References

[1] J.L. Anderson, D.A. Morrow, Acute myocardial infarction, N. Engl. J. Med. 376 (21) (2017) 2053–2064.
[2] G. Heusch, B.J. Gersh, The pathophysiology of acute myocardial infarction and strategies of protection beyond reperfusion: a continual challenge, Eur. Heart J. 38 (11) (2017) 774–784.
[3] G.M. Fröhlich, P. Meier, S.K. White, D.M. Yellon, D.J. Hausenloy, Myocardial reperfusion injury: looking beyond primary PCI, Eur. Heart J. 34 (23) (2013) 1714–1722.
[4] P.G. Steg, A. Kerner, G.B.J. Mancini, H.R. Reynolds, A.C. Carvalho, V. Fridrich, H. D. White, S.A. Forman, G.A. Lamas, J.S. Hochman, C.E. Buller, O.A.T. Investigators, Impact of collateral flow to the occluded infarct-related artery on clinical outcomes in patients with recent myocardial infarction: a report from the randomized occluded artery trial, Circulation 121 (25) (2010) 2724–2730.
[5] A. von Gise, W.T. Pu, Endocardial and epicardial epithelial to mesenchymal transitions in heart development and disease, Circ. Res. 110 (12) (2012) 1628–1645.
[6] S. Liu, X. Chen, L. Bao, T. Liu, P. Yuan, X. Yang, X. Qiu, J.J. Gooding, Y. Bai, J. Xiao, F. Pu, Y. Jin, Treatment of infarcted heart tissue via the capture and local delivery of circulating exosomes through antibody-conjugated magnetic nanoparticles, Nat. Biomed. Eng. 4 (11) (2020) 1063–1075.
[7] X. Liang, Y. Ding, F. Lin, Y. Zhang, X. Zhou, Q. Meng, X. Lu, G. Jiang, H. Zhu, Y. Chen, Q. Lian, H. Fan, Z. Liu, Overexpression of ERBB4 rejuvenates aged mesenchymal stem cells and enhances angiogenesis via PI3K/AKT and MAPK/ERK pathways, Faseb. J. 33 (3) (2019) 4559–4570.
[8] L. Luo, J. Tang, K. Nishi, C. Yan, P.-U. Dinh, J. Cores, T. Kudo, J. Zhang, T.-S. Li, K. Cheng, Fabrication of synthetic mesenchymal stem cells for the treatment of acute myocardial infarction in mice, Circ. Res. 120 (11) (2017) 1768–1775.
[9] M. Desgres, P. Menasché, Clinical translation of pluripotent stem cell therapies: challenges and considerations, Cell Stem Cell 25 (5) (2019) 594–606.
[10] N. Beohar, J. Rapp, S. Pandya, D.W. Losordo, Rebuilding the damaged heart: the potential of cytokines and growth factors in the treatment of ischemic heart disease, J. Am. Coll. Cardiol. 56 (16) (2010) 1287–1297.
[11] N. Smart, C.A. Risebro, A.A.D. Melville, K. Moses, R.J. Schwartz, K.R. Chien, P. R. Riley, Thymosin β4 induces adult epicardial progenitor mobilization and neovascularization, Nature 445 (7124) (2007) 177–182.
[12] L.L.Y. Chiu, M. Radisic, Controlled release of thymosin β4 using collagen–chitosan composite hydrogels promotes epicardial cell migration and angiogenesis, J. Contr. Release 155 (3) (2011) 376–385.
[13] L. Ye, P. Zhang, S. Duval, L. Su, Q. Xiong, J. Zhang, Thymosin β4 increases the potency of transplanted mesenchymal stem cells for myocardial repair, Circulation 128 (11 Suppl 1) (2013) S32–S41.
[14] S.H. Tan, S.J. Loo, Y. Gao, Z.H. Tao, L.P. Su, C.X. Wang, S.L. Zhang, Y.H. Mu, Y. H. Cui, D. Abdurrachim, W.H. Wang, J. Lalic, K.C. Lim, J. Bu, R.S. Tan, T.H. Lee, J. Zhang, L. Ye, Thymosin β4 increases cardiac cell proliferation, cell engraftment, and the reparative potency of human induced-pluripotent stem cell-derived cardiomyocytes in a porcine model of acute myocardial infarction, Theranostics 11 (16) (2021) 7879–7895.
[15] J. Sun, H. Shen, L. Shao, X. Teng, Y. Chen, X. Liu, Z. Yang, Z. Shen, HIF-1α overexpression in mesenchymal stem cell-derived exosomes mediates cardioprotection in myocardial infarction by enhanced angiogenesis, Stem Cell Res. Ther. 11 (1) (2020), 373–373.
[16] H. Zhang, J. Wu, J. Wu, Q. Fan, J. Zhou, J. Wu, S. Liu, J. Zang, J. Ye, M. Xiao, T. Tian, J. Gao, Exosome-mediated targeted delivery of miR-210 for angiogenic therapy after cerebral ischemia in mice, J. Nanobiotechnol. 17 (1) (2019) 29.
[17] S. Liu, J. Chen, J. Shi, W. Zhou, L. Wang, W. Fang, Y. Zhong, X. Chen, Y. Chen, A. Sabri, S. Liu, M1-like macrophage-derived exosomes suppress angiogenesis and exacerbate cardiac dysfunction in a myocardial infarction microenvironment, Basic Res. Cardiol. 115 (2) (2020) 22.
[18] F. Lin, Z. Zeng, Y. Song, L. Li, Z. Wu, X. Zhang, Z. Li, X. Ke, X. Hu, YBX-1 mediated sorting of miR-133 into hypoxia/reoxygenation-induced EPC-derived exosomes to increase fibroblast angiogenesis and MEndoT, Stem Cell Res. Ther. 10 (1) (2019), 263–263.
[19] Q. Chen, M. Huang, J. Wu, Q. Jiang, X. Zheng, Exosomes isolated from the plasma of remote ischemic conditioning rats improved cardiac function and angiogenesis after myocardial infarction through targeting Hsp70, Aging (Albany NY) 12 (4) (2020) 3682–3693.
[20] E.A. Mol, Z. Lei, M.T. Roefs, M.H. Bakker, M.-J. Goumans, P.A. Doevendans, P.Y. W. Dankers, P. Vader, J.P.G. Sluijter, Injectable supramolecular ureidopyrimidinone hydrogels provide sustained release of extracellular vesicle therapeutics, Adv. Healthcare Mater. 8 (20) (2019), 1900847.
[21] C. Wang, M. Wang, T. Xu, X. Zhang, C. Lin, W. Gao, H. Xu, B. Lei, C. Mao, Engineering bioactive self-healing antibacterial exosomes hydrogel for promoting

chronic diabetic wound healing and complete skin regeneration, Theranostics 9 (1) (2019) 65–76.
[22] H. Xu, M. Sun, C. Wang, K. Xia, S. Xiao, Y. Wang, L. Ying, C. Yu, Q. Yang, Y. He, A. Liu, L. Chen, Growth differentiation factor-5–gelatin methacryloyl injectable microspheres laden with adipose-derived stem cells for repair of disc degeneration, Biofabrication 13 (1) (2020), 015010.
[23] W.J. Seeto, Y. Tian, S. Pradhan, P. Kerscher, E.A. Lipke, Rapid production of cell-laden microspheres using a flexible microfluidic encapsulation platform, Small 15 (47) (2019), 1902058.
[24] C. Zhao, S. Tian, Q. Liu, K. Xiu, I. Lei, Z. Wang, P.X. Ma, Biodegradable nanofibrous temperature-responsive gelling microspheres for heart regeneration, Adv. Funct. Mater. 30 (21) (2020), 2000776.
[25] J. Yang, Y. Zhu, F. Wang, L. Deng, X. Xu, W. Cui, Microfluidic liposomes-anchored microgels as extended delivery platform for treatment of osteoarthritis, Chem. Eng. J. 400 (2020), 126004.
[26] K.-G. Shyu, M.-T. Wang, B.-W. Wang, C.-C. Chang, J.-G. Leu, P. Kuan, H. Chang, Intramyocardial injection of naked DNA encoding HIF-1α/VP16 hybrid to enhance angiogenesis in an acute myocardial infarction model in the rat, Cardiovasc. Res. 54 (3) (2002) 576–583.
[27] J.R. Resar, A. Roguin, J. Voner, K. Nasir, T.A. Hennebry, J.M. Miller, R. Ingersoll, L. M. Kasch, G.L. Semenza, Hypoxia-Inducible factor 1α polymorphism and coronary collaterals in patients with ischemic heart disease, Chest 128 (2) (2005) 787–791.
[28] I. Ferrin, I. Beloqui, L. Zabaleta, J.M. Salcedo, C. Trigueros, A.G. Martin, Isolation, Culture, and Expansion of Mesenchymal Stem Cells, in: J.M. Crook, T.E. Ludwig (Eds.), Stem Cell Banking: Concepts and Protocols, Springer New York, New York, NY, 2017, pp. 177–190.
[29] J. Chen, D. Huang, L. Wang, J. Hou, H. Zhang, Y. Li, S. Zhong, Y. Wang, Y. Wu, W. Huang, 3D bioprinted multiscale composite scaffolds based on gelatin methacryloyl (GelMA)/chitosan microspheres as a modular bioink for enhancing 3D neurite outgrowth and elongation, J. Colloid Interface Sci. 574 (2020) 162–173.
[30] J.J. Weyers, D.D. Carlson, C.E. Murry, S.M. Schwartz, W.M. Mahoney Jr., Retrograde perfusion and filling of mouse coronary vasculature as preparation for micro computed tomography imaging, JoVE 60 (2012) e3740–e3740.
[31] F.G. Kugeratski, K. Hodge, S. Lilla, K.M. McAndrews, X. Zhou, R.F. Hwang, S. Zanivan, R. Kalluri, Quantitative proteomics identifies the core proteome of exosomes with syntenin-1 as the highest abundant protein and a putative universal biomarker, Nat. Cell Biol. 23 (6) (2021) 631–641.
[32] J. Fadel Paul, Nitric oxide and cardiovascular regulation, Hypertension 69 (5) (2017) 778–779.
[33] S.F. Pedersen, S.A. Thrysøe, W.P. Paaske, T. Thim, E. Falk, S. Ringgaard, W.Y. Kim, CMR assessment of endothelial damage and angiogenesis in porcine coronary arteries using gadofosveset, J. Cardiovasc. Magn. Reson. 13 (1) (2011), 10–10.
[34] Z. He, A.Y. Chen, Y. Rojanasakul, G.O. Rankin, Y.C. Chen, Gallic acid, a phenolic compound, exerts anti-angiogenic effects via the PTEN/AKT/HIF-1α/VEGF signaling pathway in ovarian cancer cells, Oncol. Rep. 35 (1) (2016) 291–297.
[35] J.H. Hurst, William Kaelin, Peter Ratcliffe, and Gregg Semenza receive the 2016 Albert Lasker basic medical research award, J. Clin. Invest. 126 (10) (2016) 3628–3638.
[36] C. Seiler, M. Stoller, B. Pitt, P. Meier, The human coronary collateral circulation: development and clinical importance, Eur. Heart J. 34 (34) (2013) 2674–2682.
[37] C. Berry, K.P. Balachandran, P.L. L'Allier, J. Lespérance, R. Bonan, K.G. Oldroyd, Importance of collateral circulation in coronary heart disease, Eur. Heart J. 28 (3) (2007) 278–291.
[38] L. Bagno, K.E. Hatzistergos, W. Balkan, J.M. Hare, Mesenchymal stem cell-based therapy for cardiovascular disease: progress and challenges, Mol. Ther. : J. Am. Soc. Gene Ther. 26 (7) (2018) 1610–1623.
[39] C. Lo Sicco, D. Reverberi, C. Balbi, V. Ulivi, E. Principi, L. Pascucci, P. Becherini, M. C. Bosco, L. Varesio, C. Franzin, M. Pozzobon, R. Cancedda, R. Tasso, Mesenchymal stem cell-derived extracellular vesicles as mediators of anti-inflammatory effects: endorsement of macrophage polarization, STEM CELLS Transl. Med. 6 (3) (2017) 1018–1028.
[40] R.C. de Abreu, H. Fernandes, P.A. da Costa Martins, S. Sahoo, C. Emanueli, L. Ferreira, Native and bioengineered extracellular vesicles for cardiovascular therapeutics, Nat. Rev. Cardiol. 17 (11) (2020) 685–697.
[41] P. Chen, L. Wang, X. Fan, X. Ning, B. Yu, C. Ou, M. Chen, Targeted delivery of extracellular vesicles in heart injury, Theranostics 11 (5) (2021) 2263–2277.
[42] Z. Belhadj, B. He, H. Deng, S. Song, H. Zhang, X. Wang, W. Dai, Q. Zhang, A combined "eat me/don't eat me" strategy based on extracellular vesicles for anticancer nanomedicine, J. Extracell. Vesicles 9 (1) (2020), 1806444.
[43] A.K. Riau, H.S. Ong, G.H.F. Yam, J.S. Mehta, Sustained delivery system for stem cell-derived exosomes, Front. Pharmacol. 10 (2019) 1368.
[44] K. Krutkramelis, B. Xia, J. Oakey, Monodisperse polyethylene glycol diacrylate hydrogel microsphere formation by oxygen-controlled photopolymerization in a microfluidic device, Lab Chip 16 (8) (2016) 1457–1465.
[45] Q. Xiao, Y. Ji, Z. Xiao, Y. Zhang, H. Lin, Q. Wang, Novel multifunctional NaYF4:Er3+,Yb3+/PEGDA hybrid microspheres: NIR-light-activated photopolymerization and drug delivery, Chem. Commun. 49 (15) (2013) 1527–1529.
[46] A.K. Miri, D. Nieto, L. Iglesias, H. Goodarzi Hosseinabadi, S. Maharjan, G.U. Ruiz-Esparza, P. Khoshakhlagh, A. Manbachi, M.R. Dokmeci, S. Chen, S.R. Shin, Y. S. Zhang, A. Khademhosseini, Microfluidics-enabled multimaterial maskless stereolithographic bioprinting, Adv. Mater. 30 (27) (2018) e1800242–e1800242.
[47] A.L.Y. Nachlas, S. Li, B.W. Streeter, K.J. De Jesus Morales, F. Sulejmani, D. I. Madukauwa-David, D. Bejleri, W. Sun, A.P. Yoganathan, M.E. Davis, A multilayered valve leaflet promotes cell-laden collagen type I production and aortic valve hemodynamics,, Biomaterials 240 (2020), 119838–119838.
[48] X. Liang, L. Zhang, S. Wang, Q. Han, R.C. Zhao, Exosomes secreted by mesenchymal stem cells promote endothelial cell angiogenesis by transferring miR-125a, J. Cell Sci. 129 (11) (2016) 2182.
[49] X.-P. Tian, C.-Y. Wang, X.-H. Jin, M. Li, F.-W. Wang, W.-J. Huang, J.-P. Yun, R.-H. Xu, Q.-Q. Cai, D. Xie, Acidic microenvironment up-regulates exosomal miR-21 and miR-10b in early-stage hepatocellular carcinoma to promote cancer cell proliferation and metastasis, Theranostics 9 (7) (2019) 1965–1979.
[50] E. Mogilyansky, I. Rigoutsos, The miR-17/92 cluster: a comprehensive update on its genomics, genetics, functions and increasingly important and numerous roles in health and disease, Cell Death Differ. 20 (12) (2013) 1603–1614.
[51] B. Duan, S. Shi, H. Yue, B. You, Y. Shan, Z. Zhu, L. Bao, Y. You, Exosomal miR-17-5p promotes angiogenesis in nasopharyngeal carcinoma via targeting BAMBI,, J. Cancer 10 (26) (2019) 6681–6692.
[52] G. Loor, P.T. Schumacker, Role of hypoxia-inducible factor in cell survival during myocardial ischemia–reperfusion, Cell Death Differ. 15 (4) (2008) 686–690.
[53] Y.A. Minamishima, J. Moslehi, R.F. Padera, R.T. Bronson, R. Liao, W.G. Kaelin Jr., A feedback loop involving the Phd3 prolyl hydroxylase tunes the mammalian hypoxic response in vivo, Mol. Cell Biol. 29 (21) (2009) 5729–5741.
[54] P.M. Jaakkola, K. Rantanen, The regulation, localization, and functions of oxygen-sensing prolyl hydroxylase PHD3, Biol. Chem. 394 (4) (2013) 449–457.
[55] Y.-M. Tian, D.R. Mole, P.J. Ratcliffe, J.M. Gleadle, Characterization of different isoforms of the HIF prolyl hydroxylase PHD1 generated by alternative initiation, Biochem. J. 397 (1) (2006) 179–186.
[56] P. Miikkulainen, H. Högel, K. Rantanen, T. Suomi, P. Kouvonen, L.L. Elo, P. M. Jaakkola, HIF prolyl hydroxylase PHD3 regulates translational machinery and glucose metabolism in clear cell renal cell carcinoma, Cancer Metabol. 5 (2017), 5–5.
[57] C. Théry, S. Amigorena, G. Raposo, A. Clayton, Isolation and characterization of exosomes from cell culture supernatants and biological fluids, Current Protocols Cell Biol. 30 (1) (2006), 3.22.1-3.22.29.
[58] S.A. Melo, L.B. Luecke, C. Kahlert, A.F. Fernandez, S.T. Gammon, J. Kaye, V. S. LeBleu, E.A. Mittendorf, J. Weitz, N. Rahbari, C. Reissfelder, C. Pilarsky, M. F. Fraga, D. Piwnica-Worms, R. Kalluri, Glypican-1 identifies cancer exosomes and detects early pancreatic cancer, Nature 523 (7559) (2015) 177–182.
[59] Q. Lian, Y. Zhang, X. Liang, F. Gao, H.-F. Tse, Directed Differentiation of Human-Induced Pluripotent Stem Cells to Mesenchymal Stem Cells, in: M. Gnecchi (Ed.), Mesenchymal Stem Cells: Methods and Protocols, Springer New York, New York, NY, 2016, pp. 289–298.
[60] A. Thakur, X. Ke, Y.-W. Chen, P. Motallebnejad, K. Zhang, Q. Lian, H.J. Chen, The mini player with diverse functions: extracellular vesicles in cell biology, disease, Therapeut. Protein Cell (2021).
[61] A.J.C. Bloor, A. Patel, J.E. Griffin, M.H. Gilleece, R. Radia, D.T. Yeung, D. Drier, L. S. Larson, G.I. Uenishi, D. Hei, K. Kelly, I. Slukvin, J.E.J. Rasko, Production, safety and efficacy of iPSC-derived mesenchymal stromal cells in acute steroid-resistant graft versus host disease: a phase I, multicenter, open-label, dose-escalation study, Nat. Med. 26 (11) (2020) 1720–1725.